The Astrophysical Journal Letters, 929:L21 (6pp), 2022 April 20 https://doi.org/10.3847/2041-8213/ac6421

Deep Very Large Telescope Photometry of the Faint Stellar System in the Large Magellanic Cloud Periphery YMCA-1

Massimiliano Gatto[1,2], V. Ripepi[1], M. Bellazzini[3], M. Dall'ora[1], M. Tosi[3], C. Tortora[1], M. Cignoni[1,4,5], M.-R. L. Cioni[6], F. Cusano[3], G. Longo[2], M. Marconi[1], I. Musella[1], P. Schipani[1], and M. Spavone[1]
[1] INAF–Osservatorio Astronomico di Capodimonte, Via Moiariello 16, I-80131, Naples, Italy; massimiliano.gatto@inaf.it
[2] Department of Physics, University of Naples Federico II, C.U. Monte Sant'Angelo, Via Cinthia, I-80126, Naples, Italy
[3] INAF-Osservatorio di Astrofisica e Scienza dello Spazio, Via Gobetti 93/3, I-40129 Bologna, Italy
[4] Physics Departement, University of Pisa, Largo Bruno Pontecorvo, 3, I-56127 Pisa, Italy
[5] INFN, Largo B. Pontecorvo 3, I-56127, Pisa, Italy
[6] Leibniz-Institut für Astrophysik Potsdam, An der Sternwarte 16, D-14482 Potsdam, Germany
Received 2022 March 3; revised 2022 April 4; accepted 2022 April 4; published 2022 April 21

Abstract

We present FORS2@VLT follow-up photometry of YMCA-1, a recently discovered stellar system located 13° from the Large Magellanic Cloud (LMC) center. The deep color–magnitude diagram (CMD) reveals a well-defined main sequence (MS) and a handful of stars in the post-MS evolutionary phases. We analyze the YMCA-1 CMD by means of the automated isochrone-matching package `ASteCA` and model its radial density profile with a Plummer function. We find that YMCA-1 is an old ($11.7^{+1.7}_{-1.3}$ Gyr), metal-intermediate ([Fe/H] $\simeq -1.12^{+0.21}_{-0.13}$ dex), compact ($r_{\rm h} = 3.5 \pm 0.5$ pc), low-mass ($M = 10^{2.45\pm0.02} M_{\odot}$), and low-luminosity ($M_V = -0.47 \pm 0.57$ mag) stellar system. The estimated distance modulus ($\mu_0 = 18.72^{+0.15}_{-0.17}$ mag), corresponding to about 55 kpc, suggests that YMCA-1 is associated with the LMC, but we cannot discard the scenario in which it is a Milky Way satellite. The structural parameters of YMCA-1 are remarkably different compared with those of the 15 known old LMC globular clusters. In particular, it resides in a transition region of the M_V–r_h plane, in between the ultrafaint dwarf galaxies and the classical old clusters, and close to SMASH-1, another faint stellar system recently discovered in the LMC surroundings.

Unified Astronomy Thesaurus concepts: Large Magellanic Cloud (903); Star clusters (1567); Hertzsprung Russell diagram (725); Galaxy interactions (600); Broad band photometry (184); Milky Way stellar halo (1060)

1. Introduction

One of the most lively fields of modern astrophysics is the search for faint stellar systems inhabiting the Milky Way (MW) halo or the periphery of the MW satellites. Among the tens of MW satellites, the Large Magellanic Cloud (LMC) has particular relevance, as it is the largest and is known to have entered the MW halo with its own system of dwarf galaxy satellites (Kallivayalil et al. 2018). The LMC is also known to possess at least 15 globular clusters (GCs), as old as its oldest stars (i.e., 12–13 Gyr), which can be used to probe the earliest phases of its evolution. For example, based on accurate spectroscopic analysis, Mucciarelli et al. (2021) discovered that the old cluster NGC 2005 has been captured by the LMC from a smaller satellite galaxy now completely dissolved.

In recent years, thanks to the advent of deep panoramic surveys probing large portions of the sky, the number of faint stellar systems discovered in the vicinity of the Magellanic Clouds (MCs) has dramatically increased (Bechtol et al. 2015; Drlica-Wagner et al. 2015; Kim & Jerjen 2015; Koposov et al. 2015; Martin et al. 2016a; Torrealba et al. 2018; Bellazzini et al. 2019), bringing new puzzle pieces to the reconstruction of the evolutionary history of the MCs. For example, Martin et al. (2016a) reported the discovery of SMASH-1, a faint stellar system at 11°.3 in projection from the LMC center, whose properties place it in between the classical GCs and the ultrafaint dwarf galaxies (UFDs). The compactness of SMASH-1 led the authors to suggest that it likely is an old star cluster (SC) fundamentally different from UFDs, which are heavily dark-matter dominated (see, e.g., Simon 2019, and references therein). Nonetheless, the properties of SMASH-1 are very different from those shown by the historically known old LMC GCs. Indeed, unlike these objects, it is faint ($L_{\rm V} = 10^{2.3} L_{\odot}$), compact ($r_{\rm h} = 9.1$ pc), and highly elliptical in shape. Detecting these old stellar systems and unveiling their origin are of primary importance to understanding how the MCs and galaxies in general form and evolve. Here we discuss another stellar system, similar to SMASH-1, that we identified for the first time through the survey "Yes, Magellanic Clouds Again" (YMCA; PI: V. Ripepi) and dubbed YMCA-1 (Gatto et al. 2021b). YMCA is carried out with the VLT Survey Telescope (VST; Capaccioli & Schipani 2011). One of the main objectives of the survey is to discover faint stellar systems in the MC peripheries. To this aim, we performed an extensive search for unknown SCs in the periphery of the LMC by means of an automated algorithm that looks for overdensities in the sky (see Gatto et al. 2020). YMCA-1 is located at about 13° to the east of the LMC center (Gatto et al. 2021b). The analysis of the color–magnitude diagram (CMD) of YMCA-1 based on VST data, carried out by means of visual isochrone fitting, suggested that it is an old ($t > 12$ Gyr) and metal-poor ([Fe/H] ~ -2.0 dex) stellar system, while its estimated distance ($D \sim 100$ kpc) placed YMCA-1 in the outermost regions of the MW halo (see Gatto et al. 2021b). However, the available VST data, which revealed only a few stars in the red-giant branch (RGB) and in the top main sequence (MS), were not

sufficiently deep to unambiguously establish its real physical nature, mainly because we could not obtain a robust distance for the target. Indeed, given the lack of evolved distance indicators such as Horizontal Branch (HB) or Red Clump (RC) stars, the distance can only be constrained by a clear identification of the MS of the system. This can only be achieved with deep follow-up photometry. Hence, to unveil the real nature of this very interesting stellar system, we carried out deep follow-up photometry with the ESO (European Southern Observatory) very large telescope (VLT). In this Letter, we report and discuss the results obtained for YMCA-1 based on this new deep data.

2. Observations and Data Reduction

Deep photometric data for YMCA-1 were obtained with the FORS2 imager of the VLT. The observations were carried out during the nights of 2021 November 2 and 29, for the $g_{\rm HIGH}$ and $I_{\rm BESSEL}$ filters, respectively. The observations were divided into 5 subexposures of 480 s each in the $g_{\rm HIGH}$ filter and 13 subexposures of 240 s each in the $I_{\rm BESSEL}$ band to reach faint magnitudes without saturating the bright members of YMCA-1. The typical seeing was of $0\farcs51$ and $0\farcs72$ in g and I, respectively. For the setup of FORS2, we chose a pixel scale of $0\farcs25$ pixel^{-1} with a field of view $6\farcm8 \times 6\farcm8$. FORS2 is equipped with a mosaic of two $2{\rm k} \times 4{\rm k}$ MIT CCDs.[7] As the dimension of YMCA-1 is much smaller than the FoV of each of the two CCDs of FORS2, we decided to place the target only on the top CCD, which has a larger FoV than the bottom one. We adopted a dithering procedure between the different subexposures to eliminate cosmic rays and bad pixels. The images were prereduced (debiasing and flat-fielding) using the standard procedures with the `IRAF` package (Tody 1986, 1993). To obtain the photometry, we adopted the DAOPHOT/ALLFRAME packages (Stetson 1987, 1994). which are best suited to reach faint magnitudes in a relatively crowded field such as YMCA-1. In brief, the different steps of the procedure were the following:

1. A quadratically varying PSF was modeled by letting the code free to adopt the function, which minimized the χ^2 of the fit. The most used function was Moffat25, while in some cases the algorithm chose the Penny1 or the Penny2 functions. A World Coordinate System (WCS) plate solution was computed for each individual image by querying the astroquery.astrometry_net Python module. Then, the stars' *XY* positions were converted to WCS coordinates by using the WCSCTRAN command, available under IRAF.
2. A stack of all the subexposures was created with MONTAGE2 (Stetson 1987, 1994) to obtain a master list of sources on the image as deep as possible.
3. ALLFRAME was run on all the subexposures using the derived master list as input for the stars' position
4. DAOMATCH/DAOMASTER (Stetson 1987, 1994) were used to match the 5 and 13 different photometric catalogs obtained for each exposure of the $g_{\rm HIGH}$ and $I_{\rm BESSEL}$ filters. Finally, the catalog in the two bands was put together.

[7] See the manual at http://www.eso.org/sci/facilities/paranal/instruments/fors/doc/VLT-MAN-ESO-13100-1543_P01.pdf.

The absolute photometric calibration was obtained by means of the stars in common with the VST catalog of the tile in which YMCA-1 resides, namely the tile YMCA 9_47. In particular, we cross-matched the PSF photometric catalog with the VST data by adopting a search radius of $0\farcs5$. Then we corrected for the color dependence of the zero points in the g and i filters.[8] Before exploiting the YMCA-1 photometric catalog obtained as described above, we applied a cleaning procedure to remove undesired extended sources and the remaining few spurious detections. To this aim, we used the SHARPNESS parameter of the DAOPHOT package, retaining only sources having $-0.15 < {\rm SHARPNESS} < 0.15$.

3. Analysis

The first step of the analysis consisted of estimating the center of YMCA-1 by means of a technique based on the Kernel Density Estimation (KDE) algorithm (see Section 3.1 in Gatto et al. 2021a for full details). As a result, the coordinates (J2000) of the YMCA-1 center are (R.A., decl.) = ($110\fdg8378$, $-64\fdg8319$). The left panel of Figure 1 shows a sky map of the region (radius = $1'$) around the YMCA-1 center, while the central panel displays a density map of the same region, smoothed by means of a Gaussian function with bandwidth = $0\farcm05$. There is a remarkable over-density of stars with respect to YMCA-1's surroundings, clearly asserting the presence of a stellar system. These maps also suggest that YMCA-1 might be slightly elongated in the northwest–southeast direction. To explore this possibility, we adopted the same method used by Martin et al. (2016b) to estimate (among the other parameters) the ellipticity and position angle of SMASH-1 (Martin et al. 2016a). However, the resulting probability density function of the ellipticity and position angle were unconstrained, and therefore, in the following we employ a conservative approach, ignoring any possible elongation in the analysis of YMCA-1. The right panel of Figure 1 displays the radial density profile (RDP; number of stars per arcminute squared) of YMCA-1 built by using concentric shells of $0\farcm05$ size. We modeled the RDP with a Plummer (1911) profile, whose analytic form is the following:

$$n(r) = \frac{n_0 \cdot r_{\rm h}^4}{(r_{\rm h}^2 + r^2)^2} + N_{\rm bkg}, \quad (1)$$

where n_0 is the central surface density, $r_{\rm h}$ is the half-light radius, and $N_{\rm bkg}$ is the estimated level of the background density. The free parameters of the model are n_0, $r_{\rm h}$, and $N_{\rm bkg}$. To fit the model to the data we adopted the `curve_fit` routine of the `scipy` Python library, which allows us to estimate the best parameters of Plummer's model through a nonlinear least-squares method. The outcomes of the fit are labeled in Figure 1 (right panel). In particular, the half-light radius $r_{\rm h}$ is an important parameter to select in an objective way stars likely members of YMCA-1.

In Figure 2 (left panel), we display the CMD of YMCA-1 within a radius $R = 0\farcm43$ around its center, corresponding to twice the half-light radius $r_{\rm h}$. The right panel of Figure 2 displays the CMD of a representative local field, taken at $1'$ from the YMCA-1 center and having an area as large as the

[8] We obtained the following calibration equations: $g = g_{\rm HIGH} + 9.656 \pm 0.005 - (0.033 \pm 0.004)(g_{\rm HIGH} - I_{\rm BESSEL})$ and $i = I_{\rm BESSEL} + 8.675 \pm 0.004 + (0.0946 \pm 0.003)(g_{\rm HIGH} - I_{\rm BESSEL})$.

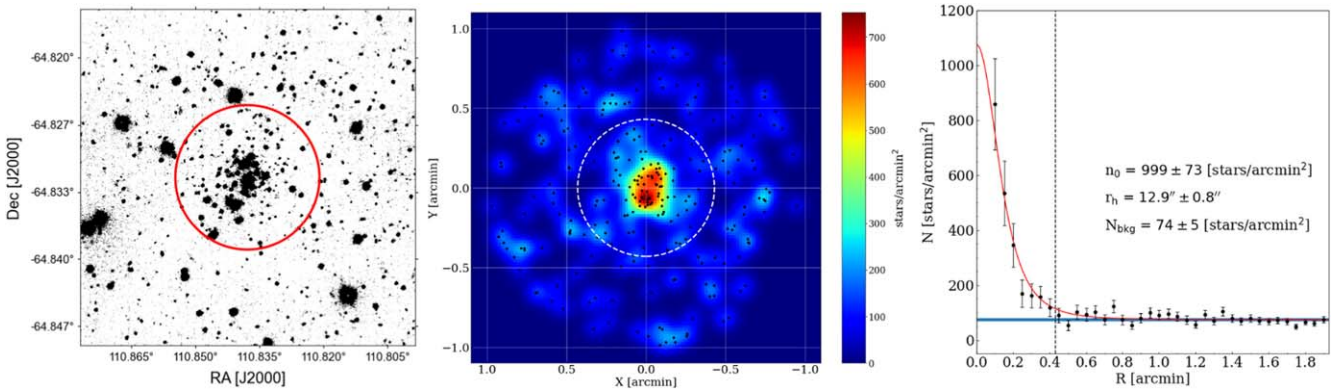

Figure 1. Left: sky image of a region of radius $R = 1'$ around the YMCA-1 center. The red circle indicates the area defined by $2r_h = 0'.43$. Center: density map of stars' relative positions with respect to the YMCA-1 center in a circular region of $1'$ in radius. We used a Gaussian function with $\sigma = 0'.05$ to smooth the map. Black points indicate the position of the stars, while the white dashed circle marks a radius $R = 0'.43$, namely twice the estimated half-light radius. Right: radial density profile of YMCA-1. Each point represents the density of stars in shells having a radius of $0'.05$. Errors are Poissonian. The red solid line is the best fit of a Plummer model as indicated in the text, whose parameters are indicated at the center of the figure. The horizontal blue strip region marks the $N_{bkg} \pm 1\sigma$ estimated values. The vertical dashed line is at $R = 0'.43$, namely $2r_h$.

area adopted in the left panel. In the background of both panels of the same figure, we show the stars observed with the VST in a region of $30'$ around YMCA-1. The CMD of YMCA-1 shows a well-defined MS, which extends below $g = 26$ mag, which is at least 2.5 mag below the turnoff (TO), while the morphology for $g < 24$ mag is similar to that depicted by the VST data. The comparison with the field provides further confirmation of the physical reality of YMCA-1. To exploit our deep CMD we adopted the Automated Stellar Cluster Analysis package (ASteCA; Perren et al. 2015), which allows us to perform an automated search of the best isochrone model that matches the data. In particular, ASteCA compares the position of the stars in the CMD with those of synthetic generated single stellar populations (SSP), adopting a genetic algorithm to find the best solution (see Perren et al. 2015, for full details). We ran ASteCA on a set of PARSEC isochrone models (Bressan et al. 2012) to estimate the age, reddening, metallicity, and distance modulus values of YMCA-1 and their uncertainties. To speed up the operations with the ASteCA package, we feed it with realistic priors, namely $t \geqslant 10$ Gyr, $E(B-V) \leqslant 0.3$ mag, $10^{-3} \leqslant Z \leqslant 10^{-1}$, and $18.0 \leqslant (m-M) \leqslant 19.50$ mag. The results of the application of ASteCA are listed in Table 1. The isochrone with the best-fitting parameters is overlaid on the data in the left panel of Figure 2. The ASteCA fit provides a distance modulus $\mu_0 = 18.72^{+0.15}_{-0.17}$ mag, which corresponds to about 55 kpc, a significantly smaller value compared to the ∼100 kpc estimated with the shallower VST photometry (Gatto et al. 2021b). Similar to the analysis with VST data, we find that the age of YMCA-1 is $t \sim 11.7^{+1.7}_{-1.3}$ Gyr, but with a higher metallicity ([Fe/H] $\simeq -1.12^{+0.21}_{-0.13}$ dex).[9] It is confirmed that YMCA-1 is a compact ($r_h = 3.5 \pm 0.5$ pc) stellar system.

Figure 2 also shows that the average MSTO of the LMC field stars, shown as gray points in the CMDs, seems to be brighter compared to that of YMCA-1. As the LMC stellar population at the outer rim of the LMC disk should also be old and metal poor (Mazzi et al. 2021), we speculate that the magnitude difference between the LMC and YMCA-1 MSTOs arises from a different distance modulus. The currently adopted distance for the LMC center is ∼49.6 kpc (e.g., Pietrzyński et al. 2019), which corresponds to a distance modulus of DM ∼ 18.49 mag, but the LMC disk is inclined in such a way that the northeast side (i.e., where YMCA-1 resides) is closer to us (e.g., Choi et al. 2018).[10] Therefore, YMCA-1 should be placed well behind the LMC main disk.

4. Discussion

The estimated distance of YMCA-1 suggests that it is likely associated with the LMC. Indeed, its three-dimensional distance from the LMC is ∼13 kpc, well within the LMC tidal radius (i.e., ∼16 kpc measured by van der Marel & Kallivayalil 2014). However, the possibility that YMCA-1 is incidentally projected beyond the LMC but not physically associated with this galaxy cannot be ruled out yet, as we still lack radial velocity measurements of its member stars.

To further investigate the YMCA-1 properties, it is useful to compare them with those of SMASH-1, which appears to have close similarities with YMCA-1. To this aim, we first estimate the total luminosity and the stellar mass of YMCA-1 with a technique similar to that described in Gatto et al. (2021b). In brief, we adopted a synthetic SSP with $t \simeq 11.7$ Gyr and [Fe/H] $\simeq -1.12$ dex (corresponding to the best isochrone found with ASteCA) constructed by means of the PARSEC isochrones.[11] Then, we measure the total luminosity and total mass of the synthetic SSP with a comparable number of MS stars as observed in YMCA-1. In particular, we consider only YMCA-1 MS stars in the magnitude interval $23.5 \leqslant g \leqslant 25$ and with a maximum color distance of 0.2 mag from the best isochrone (i.e., 24 ± 5 YMCA-1 stars by adopting the estimated $r_h = 0'.43$). The bright limit was set to select only MS stars, avoiding the use of the much less populated subgiant branch (SGB) and RGB phases. The faint-magnitude limit, instead, was chosen to take into account that at a fainter level, the completeness problems could become significant. After 500 random extractions, we estimated a total luminosity for YMCA-1 equal to $L_g = 10^{2.1 \pm 0.3} L_\odot$ and $L_i = 10^{2.1 \pm 0.4} L_\odot$ and a total mass of $M = 10^{2.45 \pm 0.02} M_\odot$.

[9] We adopted the PARSEC $Z_\odot = 0.0152$ value.

[10] There is not an estimate of the LMC distance at the YMCA-1 sky position.

[11] http://stev.oapd.inaf.it/cgi-bin/cmd

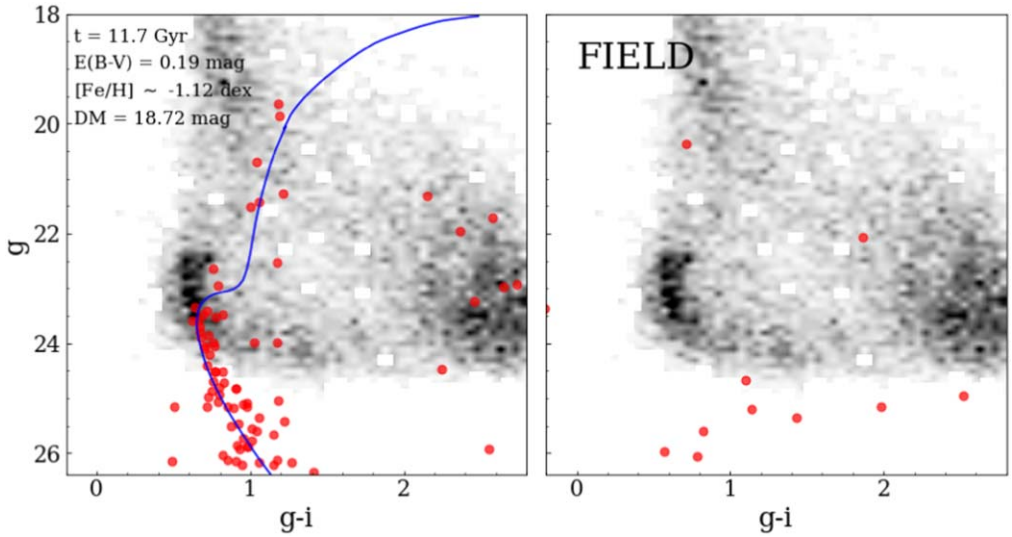

Figure 2. Left: stars whose photometry was obtained with the VLT (red points) within $r_h = 0'.43$ from the YMCA-1 center. In the background, as gray points, the stars whose photometry was obtained with the VST and within 30′ from YMCA-1 center. The blue solid line represents the best isochrone found with the ASteCA Python package matching YMCA-1 stars, whose parameters are reported in the top-left corner. Right: same as the left panel, but the red points are stars of a representative local field, which is a shell having an inner radius of 1′ and an outer radius set in order to have the same area adopted in the left panel.

Table 1
Properties of YMCA-1

Property	Value
R.A. (J2000)	$110.^{\circ}8378$
decl. (J2000)	$-64.^{\circ}8319$
Age	$11.7^{+1.7}_{-1.3}$ Gyr
μ_0	$18.72^{+0.15}_{-0.17}$ mag
[Fe/H]	$-1.12^{+0.21}_{-0.13}$ dex
$E(B-V)$	$0.19^{+0.04}_{-0.02}$ mag
Mass	$10^{2.45\pm0.02} M_{\odot}$
r_h	3.5 ± 0.5 pc
L_g	$10^{2.1\pm0.3} L_{\odot}$
L_i	$10^{2.1\pm0.4} L_{\odot}$
M_g	-0.18 ± 0.50 mag
M_i	-0.83 ± 0.55 mag
M_V	-0.47 ± 0.57 mag

In Figure 3 we display the luminosity (M_V[12]) and half-light radius of YMCA-1 and SMASH-1, in comparison with those of old LMC GCs for which structural parameters were available in the literature, and dwarf spheroidal galaxies (dSph) as well as UFDs from Simon (2019). The figure also shows the position of the old MW GCs, the parameters of which were taken from Baumgardt & Hilker (2018) and Harris (1996) (see also the caption of Figure 3). The proximity of YMCA-1 and SMASH-1 in this diagram is noticeable. Both stellar systems lie in the region of the M_V versus r_h space occupied by some peculiar faint MW GCs, such as AMR 4, Palomar 1, Koposov 1, and Koposov 2, and also near objects with difficult classification but suspected to be at the faint end of the UFD distribution. Even more interesting is the difference between YMCA-1 and the known old LMC GCs, which are located in a completely

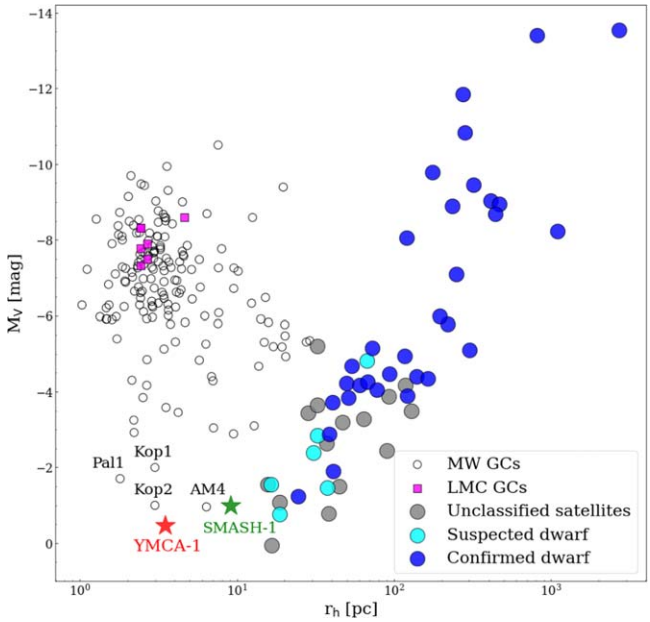

Figure 3. M_V vs. r_h in which we depict the position of YMCA-1 and SMASH-1 (colored stars), some old LMC GCs (magenta squares; r_h taken from Piatti & Mackey 2018 and M_V taken from Mackey & Gilmore 2003), and MW GCs (empty circles; taken from the Baumgardt & Hilker 2018 catalog and from Koposov et al. 2007) in this plane. We retrieved reddening values from Harris (1996, 2010 version, with some exceptions as listed in Table 1 of Gatto et al.2021b)). Finally, we also indicate the position of some confirmed and probable dwarfs (colored circles) reported in Supplementary Table 1 in Simon (2019).

different locus of the M_V versus r_h plane. They are several orders of magnitude more luminous and reside in the same parameter region occupied by the majority of the MW GCs. Therefore, YMCA-1 and SMASH-1 might belong to a peculiar subclass of stellar systems within the LMC whose properties are in between the classical GCs and the UFDs. Unlike the more massive GCs, these low-dense objects are more sensitive to the external tidal fields and hence can be subject to complete disruption, which might explain the scarcity of these stellar

[12] To estimate M_V of YMCA-1, we first transformed L_g and L_i into M_g and M_i. Then we used the following color transformation: $V = g - (0.361 \pm 0.002)$ $[(g-i) - 1.0] - (0.423 \pm 0.001)$ with rms = 0.024 mag. This equation was derived using several thousands of stars in the outskirts of the MCs having V g i data from the APASS (The AAVSO Photometric All-Sky Survey) survey (https://www.aavso.org/apass).

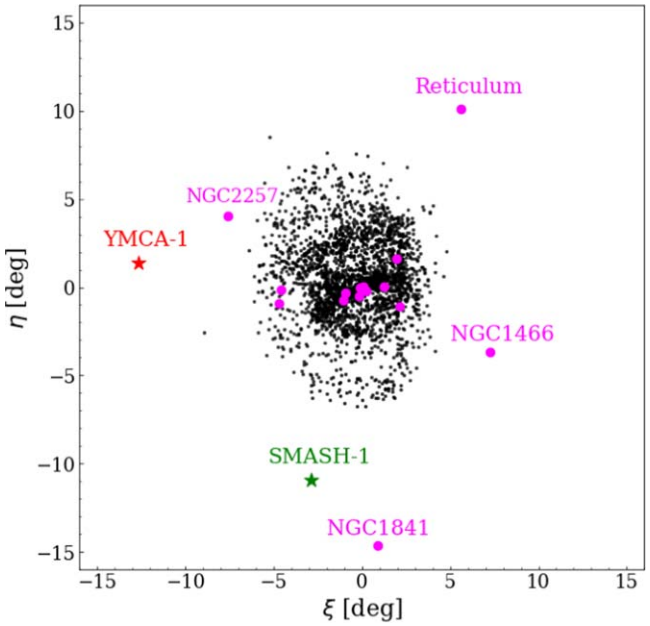

Figure 4. Relative position with respect to the LMC center of the SCs present in the Bica et al. (2008) catalog (black dots), old GCs (magenta points), and YMCA-1 and SMASH-1. Names of the outermost old GCs are also reported in the figure.

systems in the LMC. Indeed, Martin et al. (2016a) concluded that SMASH-1 is experiencing an ongoing tidal disruption, based on its strong ellipticity and its estimated tidal radius. Of course, other faint LMC-bound systems could still lie undiscovered in the outermost regions of the LMC. Finally, Figure 4 shows the relative position of the LMC SCs with respect to the LMC center. The picture reveals that YMCA-1 and SMASH-1 are among the farthest SCs ever detected around the LMC, but they are not spatially close, as the former is found to the east of the LMC, while the latter is in the south. Moreover, YMCA-1 is superimposed on (but not necessarily associated with) a substructure recently discovered in the northeast of the LMC (i.e., the North-East Structure or NES; Gatto et al. 2022).

To summarize, YMCA-1 is likely an old LMC GC with features very similar to SMASH-1. Spectroscopic follow-up of both these interesting stellar systems can be very valuable to confirm their association with the LMC. Until such spectroscopic confirmation is obtained, we cannot discard the less likely hypothesis that YMCA-1 (and possibly SMASH-1) is instead a remote MW GC.

5. Summary

In this work we exploited the FORS2@VLT follow-up of YMCA-1, a new stellar system discovered within the context of the YMCA survey, placed at about 13° from the LMC center. The deep catalog obtained in this work ($g \sim 26.5$ mag) allowed us to definitely confirm that YMCA-1 is a real physical stellar system. The exploitation of its CMD by means of the automatic isochrone-fitting package `ASteCA` (Perren et al. 2015) and the analysis of its radial density profile reveal that YMCA-1 is an old ($t = 11.7^{+1.7}_{-1.3}$ Gyr), metal-intermediate ([Fe/H] $\simeq -1.12^{+0.21}_{-0.13}$ dex), low-mass ($M = 10^{2.45\pm0.02} M_{\odot}$), and compact ($r_h \sim 3.5 \pm 0.5$ pc) stellar system. The new estimate of the YMCA-1 distance modulus suggests that it could belong to the LMC rather than to the MW halo as supposed on the basis of previous shallower VST data (Gatto et al. 2021b). Nonetheless, the uncertainties on its distance do not allow us to definitely rule out the possibility that YMCA-1 is indeed a satellite of the MW. YMCA-1 properties are remarkably different from the ones of the 15 known old LMC GCs, as they are all very massive. As far as we are aware, only SMASH-1 (Martin et al. 2016a) exhibits properties similar to that of YMCA-1, an occurrence that might indicate they have a common origin. Spectroscopic measurements of the brightest stars belonging to YMCA-1 (and SMASH-1) with the aim of obtaining their radial velocities and evaluating their metal abundances are pivotal to assess their LMC membership and to unveil the origin of these very interesting and rare stellar systems.

We warmly thank the anonymous referee for the suggestions that helped to improve the manuscript. This work is based on Director Discretionary Time (DDT) kindly allocated by ESO to proposal 108.23LX.001 and on observations collected at the ESO within the VST Guaranteed Time Observations, Programme IDs: 0104.D-0427. M.G. and V.R. acknowledge support from the INAF fund "Funzionamento VST" (1.05.03.02.04). This work has been partially supported by INAF through the "Main Stream SSH program" (1.05.01.86.28). M.R.C. acknowledges support from the European Research Council (ERC) under the European Union's Horizon 2020 research and innovation program (grant agreement No.682115). This research was made possible through the use of the AAVSO Photometric All-Sky Survey (APASS), funded by the Robert Martin Ayers Sciences Fund and NSF AST-1412587.

Facilities: Very Large Telescope (VLT).

Software: astropy (Astropy Collaboration et al. 2013; PAstropy Collaboration et al. 2018), astroquery (Ginsburg et al. 2019), IRAF (Tody 1986, 1993), matplotlib (Hunter 2007), scikit-learn (Pedregosa et al. 2011), scipy (Virtanen et al. 2020).

ORCID iDs

Massimiliano Gatto https://orcid.org/0000-0003-4636-6457
V. Ripepi https://orcid.org/0000-0003-1801-426X
M. Bellazzini https://orcid.org/0000-0001-8200-810X
M. Dall'ora https://orcid.org/0000-0001-8209-0449
M. Tosi https://orcid.org/0000-0002-0986-4759
C. Tortora https://orcid.org/0000-0001-7958-6531
M. Cignoni https://orcid.org/0000-0001-6291-6813
M.-R. L. Cioni https://orcid.org/0000-0002-6797-696X
F. Cusano https://orcid.org/0000-0003-2910-6565
I. Musella https://orcid.org/0000-0001-5909-6615
M. Spavone https://orcid.org/0000-0002-6427-7039

References

Astropy Collaboration, Robitaille, T. P., Tollerud, E. J., et al. 2013, A&A, 558, A33
Astropy Collaboration, Price-Whelan, A. M., Sipőcz, B. M., et al. 2018, AJ, 156, 123
Baumgardt, H., & Hilker, M. 2018, MNRAS, 478, 1520
Bechtol, K., Drlica-Wagner, A., Balbinot, E., et al. 2015, ApJ, 807, 50
Bellazzini, M., Pancino, E., Ferraro, F. R., & Stetson, P. B. 2019, RNAAS, 3, 47
Bica, E., Bonatto, C., Dutra, C. M., & Santos, J. F. 2008, MNRAS, 389, 678
Bressan, A., Marigo, P., Girardi, L., et al. 2012, MNRAS, 427, 127
Capaccioli, M., & Schipani, P. 2011, Msngr, 146, 2
Choi, Y., Nidever, D. L., Olsen, K., et al. 2018, ApJ, 866, 90

Drlica-Wagner, A., Bechtol, K., Rykoff, E. S., et al. 2015, ApJ, 813, 109
Gatto, M., Ripepi, V., Bellazzini, M., et al. 2022, arXiv:2203.13298
Gatto, M., Ripepi, V., Bellazzini, M., et al. 2020, MNRAS, 499, 4114
Gatto, M., Ripepi, V., Bellazzini, M., et al. 2021b, RNAAS, 5, 159
Gatto, M., Ripepi, V., Bellazzini, M., et al. 2021a, MNRAS, 507, 3312
Ginsburg, A., Sipőcz, B. M., Brasseur, C. E., et al. 2019, AJ, 157, 98
Harris, W. E. 1996, AJ, 112, 1487
Hunter, J. D. 2007, CSE, 9, 90
Kallivayalil, N., Sales, L. V., Zivick, P., et al. 2018, ApJ, 867, 19
Kim, D., & Jerjen, H. 2015, ApJL, 808, L39
Koposov, S., de Jong, J. T. A., Belokurov, V., et al. 2007, ApJ, 669, 337
Koposov, S. E., Belokurov, V., Torrealba, G., & Evans, N. W. 2015, ApJ, 805, 130
Mackey, A. D., & Gilmore, G. F. 2003, MNRAS, 338, 85
Martin, N. F., Jungbluth, V., Nidever, D. L., et al. 2016a, ApJL, 830, L10
Martin, N. F., Ibata, R. A., Lewis, G. F., et al. 2016b, ApJ, 833, 167
Mazzi, A., Girardi, L., Zaggia, S., et al. 2021, MNRAS, 508, 245
Mucciarelli, A., Massari, D., Minelli, A., et al. 2021, NatAs, 5, 1247
Pedregosa, F., Varoquaux, G., Gramfort, A., et al. 2011, J Mach Learn Res, 12, 2825
Perren, G. I., Vázquez, R. A., & Piatti, A. E. 2015, A&A, 576, A6
Piatti, A. E., & Mackey, A. D. 2018, MNRAS, 478, 2164
Pietrzyński, G., Graczyk, D., Gallenne, A., et al. 2019, Natur, 567, 200
Plummer, H. C. 1911, MNRAS, 71, 460
Simon, J. D. 2019, ARA&A, 57, 375
Stetson, P. B. 1987, PASP, 99, 191
Stetson, P. B. 1994, PASP, 106, 250
Tody, D. 1986, Proc. SPIE, 627, 733
Tody, D. 1993, in ASP Conf. Ser. 52, Astronomical Data Analysis Software and Systems II, ed. R. J. Hanisch, R. J. V. Brissenden, & J Barnes (San Francisco, CA: ASP), 173
Torrealba, G., Belokurov, V., Koposov, S. E., et al. 2018, MNRAS, 475, 5085
van der Marel, R. P., & Kallivayalil, N. 2014, ApJ, 781, 121
Virtanen, P., Gommers, R., Oliphant, T. E., et al. 2020, Nat. Methods, 17, 261